


Genome-wide association study identifies variation of glucosidase being linked to natural variation of the maximal quantum yield of photosystem II

Saber Hamdani^a, Hongru Wang^b, Guangyong Zheng^a, Shahnaz Perveen^a, Mingnan Qu^a, Naveed Khan^a, Waqasuddin Khan^c, Jianjun Jiang^a, Ming Li^a, Xinyu Liu^a, Xiaocen Zhu^a, Govindjee^d, Chengcai Chu^{b,*} and Xin-Guang Zhu^{a,*} 

^aShanghai Institute of Plant Physiology and Ecology, Chinese Academy of Sciences, Shanghai, 200031, China

^bState Key Laboratory of Plant Genomics, Institute of Genetics and Developmental Biology, Chinese Academy of Sciences, Beijing, 100101, China

^cJamil-ur-Rahman Center for Genome Research, DR. Panjwani Center for Molecular Medicine and Drug Research, International Center for Chemical and Biological Sciences, University of Karachi, Karachi, 75270, Pakistan

^dDepartment of Biochemistry, Department of Plant Biology, and Center of Biophysics and Quantitative Biology, University of Illinois at Urbana Champaign, Urbana, IL, 61801, USA

Correspondence

*Corresponding authors,
e-mails: zhuxg@sippe.ac.cn,
ccchu@genetics.ac.cn

Received 19 October 2018;
revised 6 February 2019

doi:10.1111/ppl.12957

The maximum quantum yield of photosystem II (as reflected by variable to maximum chlorophyll *a* fluorescence, F_v/F_m) is regarded as one of the most important photosynthetic parameters. The genetic basis underlying natural variation in F_v/F_m , which shows low level of variations in plants under non-stress conditions, is not easy to be exploited using the conventional gene cloning approaches. Thus, in order to answer this question, we have followed another strategy: we used genome-wide association study (GWAS) and transgenic analysis in a rice mini-core collection. We report here that four single-nucleotide polymorphisms, located in the promoter region of β -glucosidase 5 (*BGlu-5*), are associated with observed variation in F_v/F_m . Indeed, our transgenic analysis showed a good correlation between *BGlu-5* and F_v/F_m . Thus, our work demonstrates the feasibility of using GWAS to study natural variation in F_v/F_m , suggesting that *cis*-element polymorphism, affecting the *BGlu-5* expression level, may, indirectly, contribute to F_v/F_m variation in rice through the gibberellin signaling pathway. Further research is needed to understand the mechanism of our novel observation.

Introduction

There are two photosystems in oxygenic photosynthesis: photosystem I (PSI) and photosystem II (PSII); the two together lead to water oxidation and NADP reduction during linear electron transport that was described by using the so-called Z-scheme (see Govindjee et al.

2017). PSII, the focus of this paper, is a membrane-bound protein complex with associated co-factors, which include chlorophyll *a* (Chl *a*), plastoquinone (PQ) and manganese (Mn). In cyanobacteria, algae and plants, PSII catalyzes light driven oxidation of water and reduction of PQ (Wydrzynski and Satoh 2005, Nelson and Yocum 2006). On the other hand, PSI, another membrane

Abbreviations – *BGlu-5*, *Oryza sativa* 1 β -glucosidase 5; CaMV, cauliflower mosaic virus; CDS, coding sequence; Chl *a*, chlorophyll *a*; CK, cytokinin; ETR, electron transport rate; F_0 , basal (initial, minimal) level of chlorophyll *a* fluorescence; F_m , maximal level of chlorophyll *a* fluorescence; F_v (F_m minus F_0), maximal variable chlorophyll *a* fluorescence; GA, gibberellin; GWAS, genome-wide association study; KO, knocked out; LD, linkage disequilibrium; MAF, minor allele frequency; M-PEA, multi-function plant efficiency analyzer; NPQ, non-photochemical quenching; OJIP transient, chlorophyll *a* fluorescence induction (where O is for F_0 , P is for peak [equivalent to F_m in saturating light] J and I are for inflections between O and P); PQ, plastoquinone; PSI, photosystem I; PSII, photosystem II; QQ, quantile–quantile; SNP, single-nucleotide polymorphism.

protein complex, oxidizes plastoquinol (PQH₂) via Cytochrome b₆f complex (Cramer and Kallas 2016), and reduces NADP (Golbeck 2006). After absorption of light, photosynthetic pigments, in the antenna complexes, are in their excited states, and they lose their energy by one of the three processes: (1) transfer of excitation energy to reaction center chlorophylls, where photochemistry occurs (Mamedov et al. 2015, Mirkovic et al. 2017), leading to photosynthesis (approximately 95%); and (2) loss of energy as heat (Demmig-Adams et al. 2014); and (3) as Chl *a* fluorescence (Papageorgiou and Govindjee 2004), the latter two together being approximately 5%. The sum of the probabilities of these three processes is equal to 1. The quantum yield Chl *a* fluorescence from PSI is weak and can be assumed to be constant, whereas that from PSII is strong and varies with time and light intensity. Thus, by measuring Chl *a* fluorescence (which is mostly from PSII), the yield of PSII photochemistry and heat dissipation in PSII antenna can be estimated (Papageorgiou and Govindjee 2004, Demmig-Adams et al. 2014). Thus, Chl *a* fluorescence measurements have been widely used in photosynthesis research, because many details related to the photosynthetic apparatus and performance can be obtained from this highly sensitive non-invasive probe (Krause and Weis 1984, Genty et al. 1989, Govindjee 1995, 2004, Xin et al. 2013, Hamdani et al. 2015).

In higher plants and algae, Chl *a* fluorescence induction curve, measured under high-intensity continuous light after a brief period of darkness, shows a characteristic OJIP induction curve (see e.g. Stirbet and Govindjee 2011). Several parameters have been derived from these fluorescence signals, among which the F_v/F_m ratio, where F_v (maximal variable fluorescence) is the difference between F_m , i.e. the maximal fluorescence level at the P level, and the F_0 , i.e. the minimal fluorescence level, has been widely used in photosynthesis research to provide information on the overall performance of plants. The F_v/F_m provides an estimate of the maximum quantum yield of PSII photochemistry (Butler 1978, Govindjee 2004). Therefore, any drop in this ratio, e.g. because of different stresses, can be interpreted as a decrease in PSII activity (Srivastava et al. 1997, Araus et al. 1998, Li et al. 2006, Faraloni et al. 2011). However, under unstressed conditions, F_v/F_m is highly conserved and usually has a value around 0.8 (Björkman and Demmig 1987).

Although there have been a large number of physiological and biophysical studies on changes in F_v/F_m , especially under stress, there have been very few reports on genetic mechanisms affecting natural variation on F_v/F_m (Yin et al. 2010). This can be attributed to the difficulty of efficiently pinpointing the genes affecting

variation on F_v/F_m using the traditional forward genetics approach. The genome-wide association study (GWAS), however, facilitated by the next-generation sequencing technology provides a unique opportunity to rapidly bridge the gap between the natural variation of phenotypic parameters with the associated genetic variation. This method has been successfully used for identifying genes that underlie natural variation of various ecological and agricultural traits (see e.g. Huang et al. 2010, Kump et al. 2011, Tian et al. 2011, Zhao et al. 2011, Huang et al. 2012). GWAS techniques have already been recognized as a useful tool to study natural variation of photosynthetic parameters (Flood et al. 2011, Lawson et al. 2012). Along this line, Flood et al. (2016) surveyed natural variation of photosynthetic parameters such as light use efficiency of PSII electron transport in *Arabidopsis thaliana* (*Arabidopsis*). In sorghum, Ortiz et al. (2017) have identified genetic regions and candidate genes that are related to the capacity of photosynthesis to cope with excess light energy under low temperature during the vegetative growth stage. Recently, Liu et al. (2018) identified potential genes related to net photosynthetic CO₂ uptake in soybean.

In the present study, by using a diverse rice collection, we first measured F_v/F_m under different conditions. Then, using GWAS, we identified single-nucleotide polymorphisms (SNPs) that were associated with variation in F_v/F_m . Finally, using Clustered Regularly Interspaced Short Palindromic Repeats (CRISPR)/Cas9 and over-expression technologies, we suggest here that *Oryza sativa* 1 β -glucosidase 5 (BGlu-5) may contribute (or be related) to natural variation in F_v/F_m presumably through *cis*-element polymorphism affecting its expression level. We also propose a mechanism linking the gibberellin (GA) signaling pathway with the natural variation of F_v/F_m . Further experiments and models are needed to understand the full potential of our novel observation.

Materials and methods

Growth conditions

We used a rice mini-core panel, which includes 199 rice accessions of different geographic origins (Agrama et al. 2009). Seeds were grown into seedlings for approximately 30 days in a soil seed bed located in Beijing (China) (39°55'N, 116° 25'E), and then the seedlings were transplanted into 12-l plastic pots containing commercial peat soil (Pindstrup Substrate 4). Chl *a* fluorescence measurements (F_v/F_m) were made on leaves of rice plants from July to the 1st week of August 2013. Furthermore, we re-planted the entire rice population in the field from June to September 2013 and

measured F_v/F_m in the field again from early August till September of that year. Finally, we chose 16 rice accessions that showed either high or low F_v/F_m values and grew them in controlled chambers under 14/10 h light/dark regime, at approximately 26°C, and a light intensity of approximately 500 $\mu\text{mol photons m}^{-2} \text{s}^{-1}$ (during the day) given at the top of the plants. For these plants, leaves were sampled after 40 days of growth and used for quantitative reverse transcription polymerase chain reaction (qRT-PCR) analysis. Two rice GA (gibberelin) mutants, i.e. *sd1* (GA-deficient, here called low GA) and *eui1-4* (GA-accumulated, here called high GA), were obtained from the authors of Luo et al. (2006) and Tong et al. (2014), and grown in controlled growth chambers for 30 days under the above-mentioned conditions.

F_v/F_m measurements

The ratio of variable fluorescence F_v (the maximum, F_m , minus the minimum F_0) to F_m , i.e. F_v/F_m , was recorded using the multi-function plant efficiency analyzer (M-PEA) (chlorophyll) fluorometer (Hansatech). For the F_v/F_m measurements, plants were first kept overnight at 24°C in darkness, and then their detached leaves were kept under complete darkness for 10 min, using leaf clips; this was done to avoid any potential light that the plant may receive before experiments. After a 10-min dark adaptation, the upper side of the detached leaves was exposed for 0.5 s with a saturating orange-red (625 nm) actinic light (5000 $\mu\text{mol photons m}^{-2} \text{s}^{-1}$), obtained from light-emitting diodes (LEDs). Measurements were repeated 3 to 4 times for each accession. In contrast to the above experiments on plants in pots, for field experiments, a pocket PEA chlorophyll fluorometer (Hansatech) was used to measure F_v/F_m . Leaves were first kept in darkness for 10 min, and then exposed for 1 s to white light (3000 $\mu\text{mol photons m}^{-2} \text{s}^{-1}$) obtained from LEDs.

One caveat we need to emphasize here is that because the pocket PEA is not equipped with far-red light source, which is usually applied to completely oxidize the PQ pool and hence obtain the 'correct' F_v/F_m value, we have used the basic setting for both 'in-pot' and 'in-field' experiments, i.e. without prior far-red light exposure. In order to test the effect of far-red pre-illumination on the F_v/F_m value, the wild-type ZH11 was treated with and without far-red pre-illumination. Our result shows that although there was a difference in the absolute values of F_v/F_m between measurements using these two conditions; however, the trend of F_v/F_m variation remained relatively the same (Fig. S1).

Fluorescence quenching analysis

Measurements for fluorescence quenching analysis were carried out using a Dual-PAM-100 instrument (Walz). We used plants that were moved from the growth chamber to the analysis chamber and kept overnight at 24°C in darkness. Then, after a 10-min dark adaptation period, the upper side of the detached leaves was exposed to a weak modulated measuring light for F_0 measurements. A saturating light pulse of 500 ms duration and a Photosynthetic Photon Flux Density of 20 000 $\mu\text{mol photons m}^{-2} \text{s}^{-1}$, obtained from 620-nm LED arrays, were given to the sample to measure F_m . After the 1st saturating pulse, a red actinic light of 900 $\mu\text{mol photons m}^{-2} \text{s}^{-1}$ was switched on for 10 min followed by a 10-min dark period. During this time, saturating pulses of light were applied every 20 s to measure F_m' (i.e. F_m in light). In order to obtain F_0' , red actinic light was switched off and far-red (720 nm) light was applied. The effective PSII quantum yield, $Y(III)$, the non-photochemical quenching (NPQ), and the electron transport rate (ETR) were calculated, as described by Kramer et al. (2004) and Klughammer and Schreiber (2008).

RNA isolation and real-time RT-PCR analysis

Total RNA was extracted from mature rice leaves with a Purelink RNA Mini Kit (Invitrogen) following manufacturer's instructions. RNA samples were reverse transcribed into cDNA using SuperScript III Reverse Transcriptase (Invitrogen) according to manufacturer's instructions. The qRT-PCR was carried out using the LightCycle480 System (Roche Applied Science). Transcript levels were normalized to that of *UBIQUITIN 5 (UBQ5, AK061988)* (internal control). Each PCR reaction was performed in triplicate, and the error bars represent the standard deviation from three PCR reactions. Statistical analyses involved the $2^{-\Delta\Delta\text{CT}}$ method (Livak and Schmittgen 2001). (For the primer sequences used, see Table S1).

GA measurement

Plants were sampled after 50 days of growth. About 0.5 g of leaves was collected for GA measurement (see Hedden and Sponsel 2015). Quantification of endogenous GA3 was performed, as described by Chen et al. (2012).

Genome-wide association study

The accessions of the rice mini-core diversity panel were genotyped by whole-genome sequencing, as described by Wang et al. (2016). In total, 2.3-M biallelic SNPs with minor allele frequency (MAF) $\geq 5\%$ were used for association mapping. In our study, we first normalized

the phenotype data with the quantile–quantile (QQ) plots norm function, using the R software. Then, we performed the GWAS analysis employing linear mixed model implemented in Genome-wide Efficient Mixed Model Analysis (GEMMA) (Wang et al. 2016). To further correct for population structure and reduce false positives, we did Principal component analysis (PCA) analysis on the population, and supplied the 1st four principle components as covariates in the GWAS analysis, as described by Wang et al. (2009). We used a permutation strategy to decide on the genome-wide significance level. After 200 repetitions, a P -value of 10^{-6} was chosen as the genome-wide significance threshold; at this threshold, the false discovery rate is less than 5%. Linkage disequilibrium (LD) analysis was conducted using the Haploview software version 4.2, and the LD blocks were created when the upper 95% confidence bounds of D' value exceeded 0.98 and the lower bounds exceeded 0.70, as described by Gabriel et al. (2002).

Plasmid construction for B Glu -5 overexpression

The promoter of cytosolic FBPase (FBPpro) is known to guide the expression of foreign genes only in the mesophyll cells of the leaf blades and leaf sheaths. This promoter was cloned into the binary plant transformation vector pHMS with single *Pst*I clone site. The *BGlu*-5 gene was amplified from the Nipponbare rice variety using primers listed in Table S1. The product was then ligated downstream of the FBPpro with BamHI-XmaI clone sites. The generated construct was verified by DNA sequencing, and then transformed into the *Agrobacterium tumefaciens* strain EHA105. The Nipponbare was transformed by the *Agrobacterium*-mediated plant tissue culture method.

Plasmid construction using the CRISPR/Cas9 technique

The codon-optimized hSpCas9 (Cong et al. 2013) was linked to the maize ubiquitin promoter (UBI) and then inserted into binary vector pCambia1300, which contains the hygromycin B phosphotransferase gene under the control of cauliflower mosaic virus (CaMV) 35S promoter. Then, a fragment containing an OsU6 promoter (Feng et al. 2013), a negative selection marker gene *ccdB*, flanked by two *Bsa*I restriction sites, and a single-guide RNA derived from pX260 (Cong et al. 2013), was inserted into this vector using in-fusion cloning kit (Takara) to produce the CRISPR/Cas9 binary vector pBGK032. The sequence targeting the coding sequence (CDS) region of *BGlu*-5 was synthesized and annealed to form the oligo adaptor. Then, the vector pBGK032 was digested by *Bsa*I and purified using DNA

purification kit (Tiangen). Finally, a ligation reaction (10 μ l) containing 10 ng of the digested pBGK032 vector and 0.05-mM oligo adaptor was carried out and directly transformed in *E. coli* competent cells to produce CRISPR/Cas9 plasmid (Fig. S2).

Plant transformation and mutation detection

The CRISPR/Cas9 plasmid was introduced into the *A. tumefaciens* strain EHA105, and the transformation of rice was done, as previously described (Nishimura et al. 2006). Genomic DNA was extracted from the transgenic plants, and the primer pairs flanking the designed target site were used for PCR amplification. The PCR products (300–500 bp) were sequenced and identified using the degenerate sequence decoding method (Ma et al. 2015).

Subcellular localization of B Glu -5

To determine the localization of B Glu -5, we generated B Glu -5-GFP fusion protein by tagging a green fluorescent protein (GFP) in the C-terminus and transiently transformed the wild tobacco (*Nicotiana benthamiana*). The CDS region of *BGlu*-5 was first amplified from a rice (Nipponbare) cDNA, and then inserted into the binary vector pCambia1302 with a CaMV 35S promoter via a homologous recombination-based seamless cloning method (GBClonart). The final plasmid was verified by sequencing. Then, the vector was transformed into *A. tumefaciens* strain GV3101. The *Agrobacterium* cells were first cultured and resuspended to an Optical Density (at 600 nm) of approximately 1.0 in a buffer (10 mM MES, 10 mM MgCl₂ and 200 mM acetosyringone, pH 5.7), and then infiltrated into young leaves by a syringe. After 36 to 48 h, the fluorescence signals in leaf pavement cells were analyzed with a Zeiss LSM880 two-photon confocal microscope. Chl *a* fluorescence was detected in the 650- to 720-nm range and used as a marker for the chloroplast. (The primer sequences for *BGlu*-5 amplification are listed in Table S1.)

Results

F_v/F_m measurement

In this study, a diversity panel of rice (*O. sativa*) mini-core accessions collected from different geographic regions was used, as grown under two different conditions from May to September 2013 (in Beijing, China). These two conditions were field growth (i.e. in-field) and outside pot growth (in-pot) condition. As mentioned in the Material and methods, F_v/F_m values were measured, using an M-PEA (Hansatech) for in-pot condition, and a pocket PEA chlorophyll fluorometer (Hansatech) for in-field condition. Under both the conditions, rice leaves at the

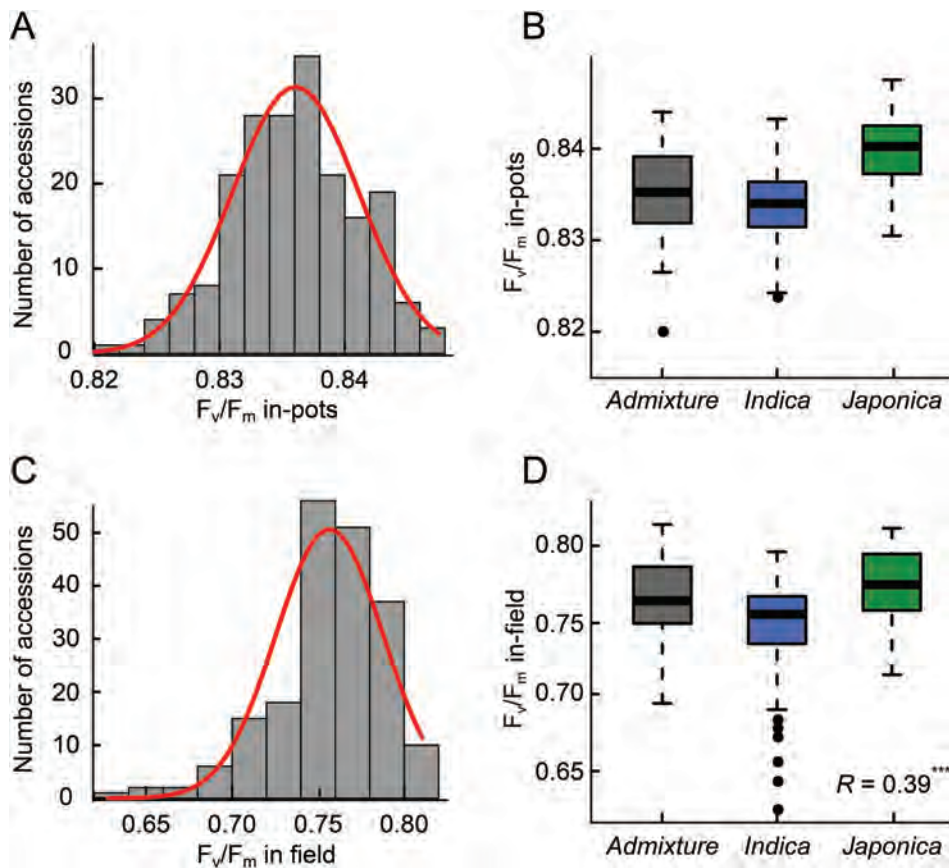


Fig. 1. Variation in F_v/F_m across rice mini-core collection. (A) Distribution of F_v/F_m variation under 'in-pots' condition. (B) Box plot representing F_v/F_m variation under in-pots condition. (C) Distribution of F_v/F_m variation under in-field condition. (D) Box plot for F_v/F_m variation under 'in-field' condition. Box edges show the upper and lower values with a median value in the middle of the box. Open dot represents the data outside the range of the box plot. *Japonica*: For the *Japonica* varietal group (TRJ, tropical; TEJ, temperate and ARO, aromatic) and *Indica*: For the *Indica* varietal group (IND, *Indica*; and AUS, aus). The Pearson's correlation coefficients (R) of the pair-wise comparison of F_v/F_m at both conditions are shown in the panel. *** P -value <0.001.

late vegetative stage to early booting stage were used. Fig. 1A shows that F_v/F_m values, measured under an in-pot condition, followed a normal distribution with a median of 0.835 (at around 65% of the population) and varied from 0.82 to 0.85 across the entire rice mini-core collection. The *Japonica* varietal group (TRJ, tropical; TEJ, temperate; and ARO, aromatic) exhibited slightly higher F_v/F_m as compared with the *Indica* varietal group (IND, *Indica* and AUS, aus) and *Admix* (Fig. 1B). In order to test the accuracy of our measurements, we re-planted the mini-core collection under in-field condition from June to September 2013 (in Beijing, China). Fig. 1C shows that around 80% of the population exhibited higher F_v/F_m than the median ($F_v/F_m = 0.725$). However, the box plot for the variation of F_v/F_m across subpopulations showed a highly similar trend as compared to those under in-pot condition ($R = 0.39$; *** $P < 0.001$), i.e. the F_v/F_m ratios observed in *Japonica* remained slightly higher than in *Indica* and *Admix* (Fig. 1D).

GWAS on F_v/F_m

In order to identify candidate genes contributing to natural variation in F_v/F_m , the accessions in the rice mini-core diversity panel were genotyped by

whole-genome sequencing, and a total of 2.3-M biallelic SNPs with $MAF \geq 5\%$ were used for association mapping. Using a linear mixed model implemented in GEMMA, we identified several SNPs that were highly associated with F_v/F_m variation (P -value $< 10^{-6}$) (Fig. 2A). The QQ plot analysis indicates that the identified SNPs represent true positive discoveries, because the observed $-\log_{10} P$ -values were higher than the expected distribution, especially in the most significant P -value range (Fig. 2B). The most significantly associated SNP (called here SNP1), which explains approximately 28% of the total phenotypic variation, was found at *Chr 1: 40840545*, with a P -value of $7.3E^{-08}$, although there were also a number of other SNPs showing high significance levels (P -values $< 10^{-6}$) (Table S2). In the current study, we focused only on SNP1 and the genes in its vicinity because it shows the highest statistical significance level (Table S2). All the candidate genes in the vicinity of this SNP and also other potential SNPs are listed in Table S2 according to the Michigan State University (MSU) rice genome database (<http://rice.plantbiology.msu.edu/>).

Using LD analysis covering 100-kb interval centered around SNP1, we identified one LD block of 11 Kb (*Chr1*:

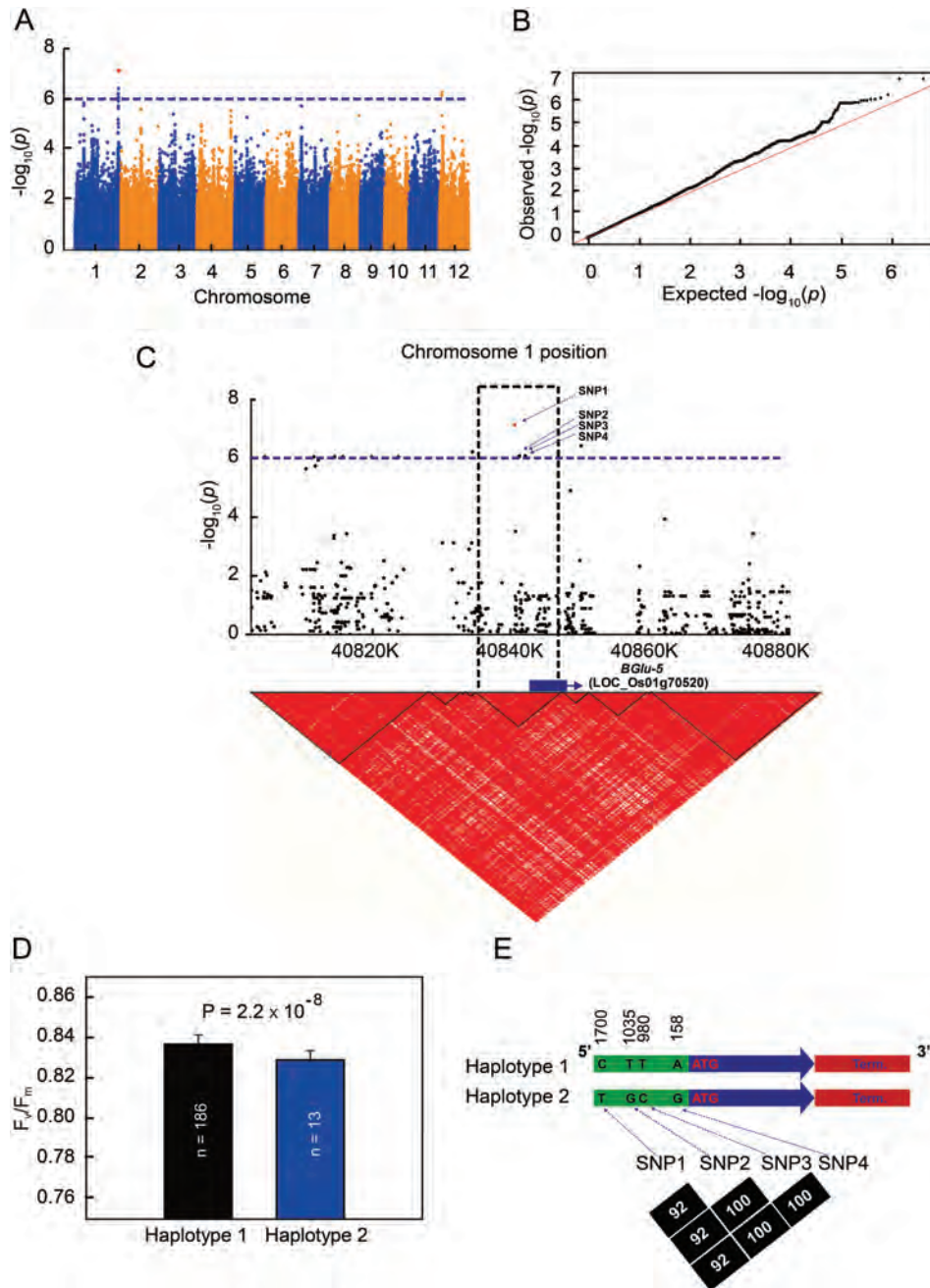


Fig. 2. Legend on next Page.

Table 1. Allelic diversity of B*Glu-5*-haplotypes across rice mini-core collection and the corresponding F_v/F_m . SNP1: Chr1: 40840545, P-value: $7.3E^{-08}$, C is the major allele. SNP2: Chr1: 40841210, P-value: $8.32E^{-07}$, T is the major allele. SNP3: Chr1: 40841265, P-value: $8.32E^{-07}$, T is the major allele. SNP4: Chr1: 40842087, P-value: $8.32E^{-07}$, A is the major allele.

Haplotypes Subgroup	SNP1	SNP2	SNP3	SNP4	F_v/F_m
Haplotype 1 (n = 186) <i>Japonica</i>	C	T	T	A	0.837 ± 0.005
Haplotype 2 (n = 13) <i>Indica/Admix/Aus</i>	T	G	C	G	0.829 ± 0.005

40835717 to 40846995) harboring SNP1. In addition, three significant SNPs, i.e. SNP2 (Chr 1: 40841210), SNP3 (Chr 1: 40841265) and SNP4 (Chr 1: 40842087) with a P-value of $8.32E^{-07}$ were located in the vicinity of SNP1 in the same LD block (Fig. 2C), providing additional evidence for this region to be a major locus associated with F_v/F_m variation. Interestingly, only one gene encoding a B*Glu-5* (LOC_Os01g70520) was found in this LD block (Fig. 2C), suggesting that this gene is a strong candidate contributing to variation in F_v/F_m , without excluding other candidate genes not located in this LD block. These other genes will be examined in the future. Furthermore, the allelic diversity of the above-mentioned SNPs across rice mini-core collection revealed two different B*Glu-5*-haplotypes, i.e. B*Glu-5*-haplotype 1 (containing major alleles: CTTA), which was represented in approximately 93% of the population, and B*Glu-5*-haplotype 2 (containing minor alleles: TGCG), which occurred in approximately 7% of the population (Table S3). Interestingly, we found that B*Glu-5*-haplotype 1 was only detected in *Japonica*; however, B*Glu-5*-haplotype 2 was detected in both *Indica* and *Admix* (Fig. 2D and Table 1). In order to check the haplotype frequency and distribution of large-scale rice genome, we further analyzed the 3000 rice genomes project. Our result shows that B*Glu-5*-haplotype 1 was

represented in approximately 97% of the population, while B*Glu-5*-haplotype 2 occurred in approximately 1% of the population. Consistent with the result obtained with the rice mini-core collection, B*Glu-5*-haplotype 2 was only detected in the *Indica* varietal group (not in *Japonica*) and *Admix* (Tables S4 and S5). Despite the wide geographic distribution of the rice mini-core accessions, accessions with B*Glu-5*-haplotype 1 showed an independent origin as compared with those with B*Glu-5*-haplotype 2. In fact, accessions with haplotype 2 mostly exist in the Indian subcontinent (South Asia), while accessions with haplotype 1 exist in all the continents (Fig. S3). This localized distribution of two B*Glu-5*-haplotypes may reflect local adaptation of photosynthetic systems to variation in environmental factors across different latitudes or altitudes. On the other hand, based on the exact chromosomal position of the above-mentioned SNPs related to B*Glu-5*, provided by MSU rice genome database, we found that these SNPs were located in the promoter region of B*Glu-5* at 1700, 1035, 980 and 158bp from the ATG starting codon (Fig. 2E). Furthermore, we found that the correlation coefficients (R^2) between these SNPs across the mini-core diversity panels varied from 92 to 100%, suggesting that these SNPs are likely inherited together (Fig. 2E).

Fig. 2. GWAS analysis and characterization of F_v/F_m trait. (A) Manhattan plot for F_v/F_m variation in a population of rice mini-core grown under in-pots condition. x-axis shows the SNPs along each chromosome; y-axis is the $-\log_{10}$ (P-value). Blue horizontal dashed line indicates a genome-wide significance threshold of $-\log_{10}$ (P-value) = 6. (B) QQ plot of the linear mixed model for F_v/F_m variation. x-axis shows the expected $-\log_{10}$ (P-value); y-axis is the observed $-\log_{10}$ (P-value). (C) Zoom view in the Manhattan plot of the genomic region harboring the highest scoring SNP (SNP1), located at Chr 1: 40840545. The positions of SNP1 (highlighted with red color), SNP2 (Chr 1: 40841210), SNP3 (Chr 1: 40841265) and SNP4 (Chr 1: 40842087) are indicated by blue dashed arrows. The pair-wise LD between SNP markers, covering 100-kb interval centered on SNP1, is indicated as D' values. Dark red for a value of 1 and white for 0. The black dashed line indicates the LD block that contains significant SNPs. The location of the candidate gene (B*Glu-5*) is indicated by blue box. (D) Maximum quantum yield of PSII, F_v/F_m , measured in rice mini-core accessions. Black histogram is for B*Glu-5*-haplotype 1, while blue histogram is for B*Glu-5*-haplotype 2. The population size (n) is shown in the figure. Values are shown as means \pm SD. (n = 186 for haplotype 1; n = 13 for haplotype 2). The P-value from a t-test is shown in the figure. (E) Schematic diagram of the B*Glu-5* gene structure. B*Glu-5*-haplotype 1, containing the major alleles (C, T, T and A) of SNPs is shown in the upper panel, while B*Glu-5*-haplotype 2, containing the minor alleles (T, G, C and G) is shown in the bottom panel. The distances between SNPs and the ATG start codon are indicated in the figure. The promoter is indicated by green box, the CDS is indicated by blue arrow and the terminator (term.) is indicated by red box. The correlation coefficient (R^2) of each pair-wise comparison of SNPs is indicated. The number in the square shows the 100-fold value of R^2 , which ranged from 0 to 100. The location of SNPs in the promoter is indicated by dashed blue line.

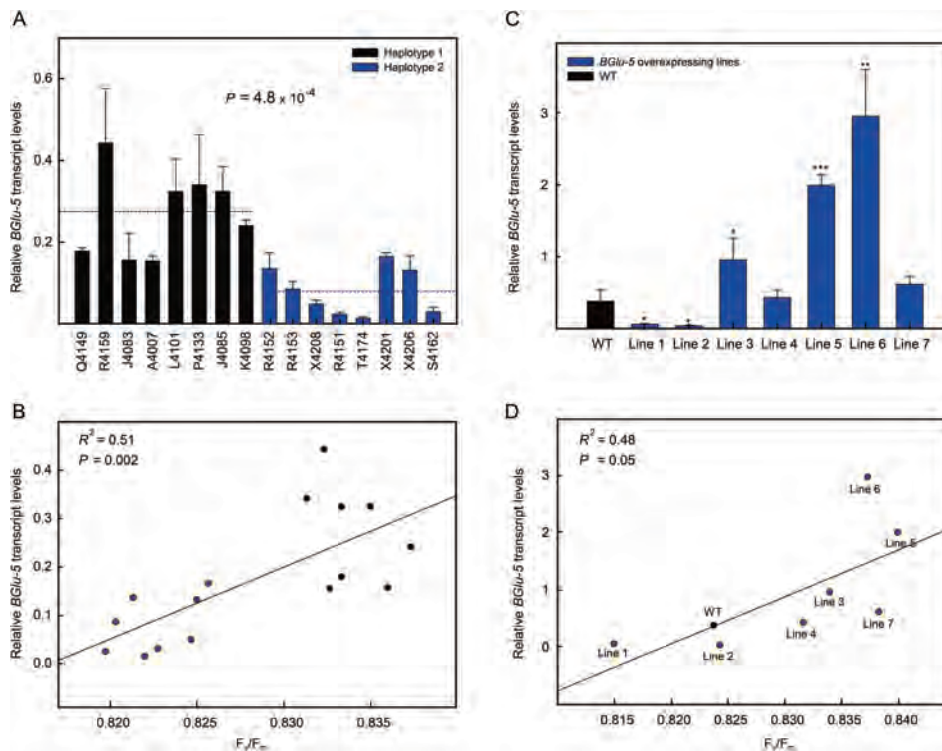


Fig. 3. *BGlu-5* transcript analysis. (A) Relative transcript levels of *BGlu-5* gene (LOC_Os01g70520) in rice mini-core accessions with *BGlu-5*-haplotype 1 (A4007, J4083, J4085, K4098, L4101, P4133, Q4149 and R4159) and *BGlu-5*-haplotype 2 (P4135, R4151, R4152, R4153, R4160, T4174, X4201 and X4208), determined by qRT-PCR. The *BGlu-5* transcript levels were normalized to that of *UBQ-5* (internal control). Black histograms are for *BGlu-5*-haplotype 1, while blue histograms are for *BGlu-5*-haplotype 2. Values are shown as means \pm sd. ($n = 3$). The P -value from a t -test, for the transcript levels of *BGlu-5*-haplotypes, is shown in the figure. (B) Correlation between F_v/F_m and *BGlu-5* relative transcript levels. Each point represents the average of three replications. The correlation coefficient (R^2) and the P -values are shown in the panel. (C) Relative transcript levels of *BGlu-5* gene (LOC_Os01g70520) in T0 rice plants overexpressing *BGlu-5* (blue histogram) and the wild-type Nipponbare (black histogram). Values are shown as means \pm sd. ($n = 3$). The asterisks indicate that the comparison between two groups is significant by Student's t -test: * $P < 0.05$ and ** $0.001 < P < 0.01$. (D) Correlation between F_v/F_m and *BGlu-5* relative transcript levels. Each point represents the average of three replications. The correlation coefficient (R^2) and the P -values are shown in the panel.

Transcription analysis of *BGlu-5*

The above results suggest that the SNPs in the promoter region of *BGlu-5* might be related to variation of F_v/F_m . One possible mechanism is that these variations of SNPs lead to different expression levels of *BGlu5* and later changes in F_v/F_m . To test this possibility, we evaluated the correlation between the expression levels of the *BGlu-5* gene and F_v/F_m . Specifically, we chose eight rice accessions, which had drastically different F_v/F_m values under different growth conditions, i.e. in-pots, in-field and in-controlled-growth chambers (Table S3). Our data show a significant difference in the *BGlu-5* expression level (P -value = $4.8E^{-4}$) between *BGlu-5*-haplotypes: haplotype 1 showed a 3.4-fold higher expression as compared with haplotype 2 (Fig. 3A). Fig. 3B shows that the relative expression level of *BGlu-5* was significantly correlated with variation in F_v/F_m in rice grown in controlled growth chamber ($R^2 = 0.51$, P -value = 0.002). This result

shows a correlation between *BGlu-5* transcription level and F_v/F_m , suggesting that this gene probably contributes to F_v/F_m variation in rice mini-core collection.

Transgenic analysis and Chl a fluorescence measurement

To further evaluate the correlation between *BGlu-5* expression and F_v/F_m , both *BGlu-5* overexpression and *BGlu-5* knockout, using CRISPR/Cas9 technologies, were used. To do this, we first developed a T0 rice plant overexpressing *BGlu-5*. Fig. 3C shows that overexpressing lines exhibited different transcriptional levels of *BGlu-5* ranging from 10-fold downregulation to 8-fold upregulation as compared to the wild-type Nipponbare. The transcript levels of *BGlu-5* were positively correlated with changes in F_v/F_m ($R^2 = 0.48$, P -value = 0.05) (Fig. 3D). We further obtained homozygous mutant lines for which the *BGlu-5* gene was knocked out (KO), i.e. *bglu-5*. The

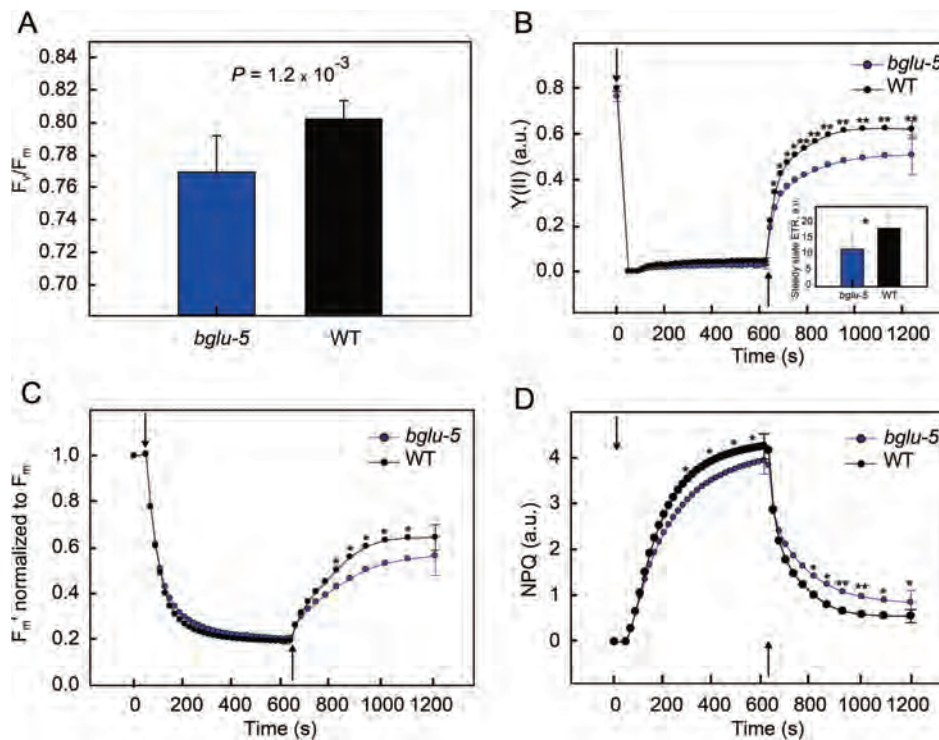


Fig. 4. Characterization of rice *bglu-5* knockout mutants. (A) Maximum quantum yield of PSII, F_v/F_m , measured in rice *bglu-5* knockout mutants (blue histogram) and the wild-type ZH11 (black histogram). The *P*-value from a *t*-test, for F_v/F_m measurements, is shown in the figure. (B) Effective quantum yield of PSII, $Y(II)$, measured in rice *bglu-5* knockout mutants (blue) and the wild-type ZH11 (black). (Inset) Steady state of ETR measured in rice *bglu-5* knockout mutants (blue histogram) and the wild-type ZH11 (black histogram). (C) Kinetics of maximum Chl fluorescence under light (F_m') normalized to F_m , measured in rice *bglu-5* knockout mutants (blue) and the wild-type ZH11 (black). (D) Kinetics of NPQ measured in rice *bglu-5* knockout mutants (blue) and the wild-type ZH11 (black). Values are shown as means \pm s.d. ($n=9$). The asterisks indicate that the comparison between two groups is significant by Student's *t*-test: * $P < 0.05$ and ** $0.001 < P < 0.01$. Arrows indicate switching on (↓) and off (↑) of the red actinic light.

CDS of *BGLU-5* was changed by a 1-bp insertion in all KO transgenic lines (Fig. S4), leading to a frame shift and subsequent loss of BGLU-5 function. As expected, we found that the KO transgenic lines exhibited a lower F_v/F_m (0.77 ± 0.01) as compared to the wild-type plants (0.8 ± 0.02) (Fig. 4A). The small ($\sim 4\%$), but significant, decrease in F_v/F_m was quite similar to that observed in *BGLU-5*-haplotypes in rice mini-core collection (Fig. 2D), providing additional evidence that BGLU-5 contributes, in some way, to the observed variation in F_v/F_m . Furthermore, KO transgenic *bglu-5* plants showed a decrease in the effective PSII quantum yield ($Y(II)$), during both light exposure and recovery in the dark, as well as in the ETR as compared to $Y(II)$ in the wild-type ZH11 plants (Fig. 4B and inset). This result suggests that BGLU-5 may influence the electron transport activity in PSII. Moreover, we showed that F_m' , i.e. F_m under light, was slightly higher, in the *bglu-5* lines as compared to that in the wild type, during light exposure (Fig. 4C); the speed of F_m' recovery after leaves were switched to low light was also slower (Fig. 4C). All these results are consistent with

the lower NPQ and slower NPQ induction during light, and slower rate of NPQ decrease in the KO transgenic lines as compared to that in the wild type (Fig. 4D). Such observed changes in fluorescence parameters suggest that the *bglu-5* KO transgenic lines are deficient in both the induction and also the recovery of photoprotection.

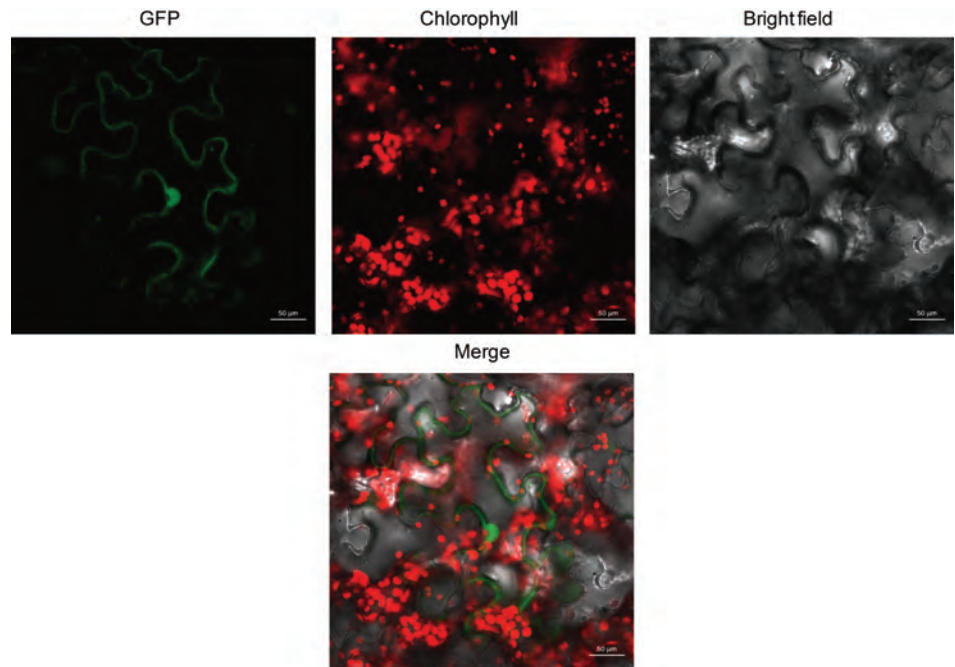
Subcellular localization of BGLU-5

We examined the subcellular localization of BGLU-5 with a BGLU-5-GFP fusion protein using pavement cells from a wild tobacco (*N. benthamiana*) plant. Our data show that BGLU-5-GFP fusion protein is localized in both the nucleus and the cytoplasm (Fig. 5). One major feature conclusion that can be deduced from this result is that BGLU-5 can only regulate F_v/F_m indirectly, because it is not in the chloroplast.

Role of GA in F_v/F_m regulation

BGLU-5 is a member of the BGLU family, which is involved in key plant developmental processes (Kleczkowski

Fig. 5. Localization BGLu-5. Sub-cellular localization of BGLu-5-GFP in the nucleus and the cytoplasm, shown in leaf pavement cells of *Nicotiana benthamiana*. Chlorophyll (middle panel) shows the chlorophyll a fluorescence detected at 650–720 nm, which is considered as a marker for the chloroplast. Scale bar, 50 μ m.



and Schell 1995), and activates phytohormones through the hydrolysis of glucoside bonds of the hormones (Wiese and Grambow 1986). Among several phytohormones targeted by BGLu, we studied three major hormones [auxin (IAA, indole acetic acid), cytokinin (CK) and GA], which are known to regulate photosynthesis, albeit indirectly (Zubo et al. 2008, Chapman and Estelle 2009, Xie et al. 2016). Fig. 6A shows changes in F_v/F_m in response to short-term hormone treatment in the *bglu-5* mutant. Results show that F_v/F_m in the *bglu-5* was restored to the wild-type level by GA treatment; however, the F_v/F_m in *bglu-5* was not altered when plants were treated with either IAA or CK (Fig. 6A). To further investigate the role of GA in F_v/F_m regulation, we measured F_v/F_m in several rice GA mutants, including *sd1* (GA-deficient, called here low GA) and *eui1-4* (GA-accumulated, called here high GA) and the wild-type ZH11. Fig. 6B shows a significant (~12%) decrease in F_v/F_m in low GA mutants (0.7 ± 0.05) as compared to that in the wild type (0.79 ± 0.02), while no change in F_v/F_m was observed in high GA mutants.

Furthermore, we measured GA levels in different rice accessions carrying either functional or non-functional BGLu-5. Fig. 6C shows higher GA levels in plants with *BGLu-5*-haplotype 1 and the wild-type ZH11 (functional BGLu-5; *BGLu-5*-haplotype 1) [0.11 ± 0.001 ng g⁻¹ fresh weight (FW) and 0.07 ± 0.001 ng g⁻¹ FW, respectively], as compared to *BGLu-5*-haplotype 2 and *bglu-5* mutant (non-functional BGLu-5) (0.025 ± 0.002 ng g⁻¹ FW and 0.023 ± 0.0005 ng g⁻¹ FW, respectively). Based on the

above results, we suggest that variation of BGLu-5 gene expression and correspondingly GA variation must have contributed, although indirectly, to the natural variation in F_v/F_m (Fig. 6D).

Discussion

In this study, we surveyed natural variation of F_v/F_m in a rice mini-core diversity panel, which includes accessions collected from different geographic origins. The variable to maximum chlorophyll a fluorescence, F_v/F_m , representing the maximal quantum yield of PSII photochemistry, is widely used in photosynthesis research, providing information on photosynthetic systems under both normal and stress conditions (see e.g. Yamane et al. 1998, Garg et al. 2002). However, given the high level of conservation of the 'light reactions' in higher plants (El-Lithy et al. 2005, Leister 2012), only a small variation of F_v/F_m exists under unstressed (normal) conditions, which hinders the progress of genetic research aiming at identifying new genes affecting changes in F_v/F_m . However, our current study shows that GWAS provide a unique opportunity to 'mine' genes controlling F_v/F_m . In this study, we have shown that there is a small but significant variation in F_v/F_m across different rice subpopulations; specifically, we found a slightly higher F_v/F_m in *Japonica* as compared to *Indica* and *Admix* varieties (Fig. 1A, B). This difference in F_v/F_m between the subpopulations was confirmed in three separate experiments, i.e. in-pots, in-field and in-growth

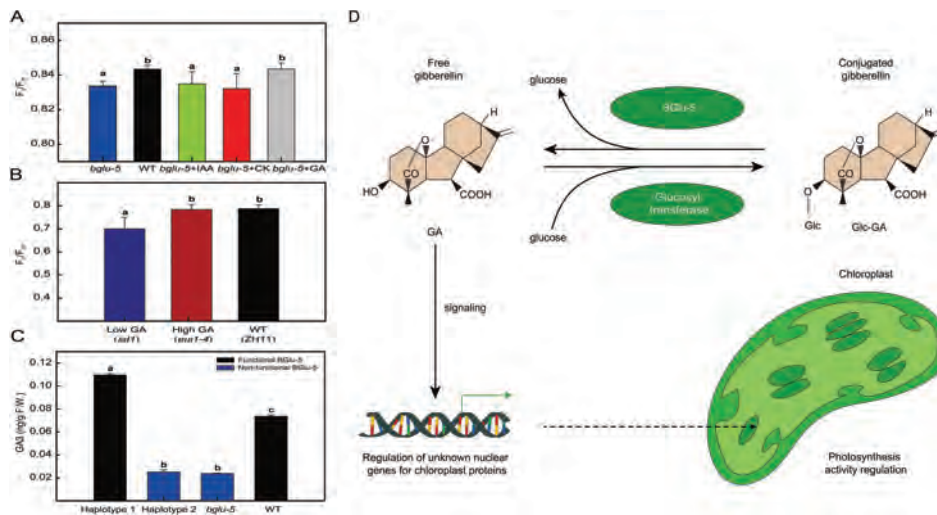


Fig. 6. Role of GA in F_v/F_m regulation. (A) Maximum quantum yield of PSII, F_v/F_m , measured in rice *bglu-5* knockout mutants (blue histogram), the wild-type ZH11 (black histogram), *bglu-5* + auxin (IAA) (green histogram), *bglu-5* + CKs (red histogram) and *bglu-5* + gibberellic acid (GA3) (gray histogram). KO transgenic plants have been sprayed by 40 μ M of phytohormones. Then, after 3 h incubation, F_v/F_m was measured ($n = 15$ for WT and *bglu-5*; $n = 8$ for the remaining samples). (B) F_v/F_m measured in rice GA mutants, i.e. *sd1* (GA-deficient, called here low GA: Blue-dark histogram), *eui1-4* (GA-accumulated, called here high GA: Red-dark histogram) and the wild-type ZH11 (black histogram). Values are shown as means \pm SD. ($n = 12$). (C) GA3 levels in functional *BGLU-5* plants (*BGLU-5*-haplotype 1 and the wild-type ZH11: Black histogram) and non-functional *BGLU-5* plants (*BGLU-5*-haplotype 2 and *bglu-5* knockout mutants: Blue histogram). ($n = 3$). For A, B, and C, values are shown as means \pm SD and lowercase letters indicate significant differences at $P \leq$.

chamber measurements (Fig. 1 and Table S3). Our results are in agreement with that of Kasajima et al. (2011) who had found a slightly higher F_v/F_m in *Japonica* as compared to *Indica* in another rice core collection. Our earlier analysis by Qu et al. (2017) showed that the heritability of F_v/F_m is 0.34. All the available evidence suggests that the small variation in F_v/F_m across rice subpopulations under unstressed condition is likely to be a non-random variation. Thus, we must conduct further genetic analysis of F_v/F_m .

The GWAS analysis of F_v/F_m , presented in this paper, revealed many significant SNPs (Fig. 2). Altogether, we had selected 20 SNPs that were highly associated with F_v/F_m variation (P -value $< 10^{-6}$), with SNP1, being the highest scoring SNP, having a P -value of $7.3E^{-08}$ (Fig. 2A and Table S2). Based on LD analysis, we have identified one LD block of 11 Kb harboring SNP1 together with three other highly significant SNPs: SNP2, SNP3 and SNP4. Because only one gene (*BGLU-5*) was found within this LD block, hence we focused on this gene in our analysis (Fig. 2C). We showed that the above-mentioned SNPs were strongly linked together, forming two *BGLU-5*-haplotypes across rice mini-core accessions. Furthermore, we found that all the four SNPs, mentioned above, were located in the promoter region of *BGLU-5* (Fig. 2E), suggesting that the observed polymorphism can influence the expression level of this gene and later influence the values of F_v/F_m . The qRT-PCR

analysis of mini-core accessions and overexpressing lines showed that *BGLU-5* had different transcriptional levels, which were correlated with the values of F_v/F_m (Fig. 3), suggesting that *BGLU-5* must have contributed, although indirectly, to natural variation of F_v/F_m .

To further confirm the correlation between *BGLU-5* and F_v/F_m variation, we had used a CRISPR/Cas9 technique to knock out *BGLU-5* in ZH11, a line commonly used in rice genetics studies. The homozygous *bglu-5* knockout lines contain a single-nucleotide insertion in the CDS region (Fig. S4), leading to a frame shift and subsequent loss of *BGLU-5* function. As expected, F_v/F_m was slightly lower in the *bglu-5* KO transgenic plants as compared to the wild type (Fig. 4A), showing similar trend as expected for the *BGLU-5*-haplotypes in the rice mini-core accessions, which have different *BGLU-5* expression levels (Fig. 2D). We note here that the observed small (approximately 4%) decrease in F_v/F_m may reflect the high degree of conservation of F_v/F_m , which can be severely affected only when a severe damage in the structural components of PSII takes place. Further measurements using the *bglu-5* show that, in addition to lower electron transport activity, there was a lower photoprotection capacity in *bglu-5* KO transgenic plants as compared to the wild type (Fig. 4). However, given that *BGLU-5* was not detected in the chloroplast (Fig. 5), we speculate that *BGLU-5* regulates F_v/F_m indirectly through intermediate steps.

Table 2. Correlation between measured F_v/F_m with the biomass-related parameters in the rice mini-core collection. The correlation coefficients and their P-values have been calculated using R function. *P-value < 0.05. **0.001 < P-value < 0.01. ***P-value < 0.001.

	F_v/F_m in-pots	Biomass	Tiller number	Grain weight /tiller	Harvest index
F_v/F_m in-field	0.39***	-0.22**	-0.26***	0.18*	0.16*
F_v/F_m in-pots	-----	-0.08	-0.23***	0.15*	0.26***

BGlu5 are ubiquitous enzymes involved in multiple physiological functions, including biomass degradation, and hydrolysis of glycolipids and oligosaccharides leading to the release of glucose. In plants, BGlu5 play an additional role in phytohormone activation by releasing glucose from the conjugated form of a hormone (Brzobohaty et al. 1993), which is considered to be a crucial step controlling many plant growth and developmental processes. We ask: does this mechanism potentially contribute to the variation in F_v/F_m ? To test the hypothesis that the slight decrease in F_v/F_m in *bglu-5* KO transgenic lines was due to decreased level of BGlu-5, which results in lower free-hormone levels, we had supplied exogenous IAA, CK and GA on *bglu-5* for a short-term treatment. Our results show that only GA treatment can recover the F_v/F_m value in the *bglu-5* to the WT level (Fig. 6A). Our results are consistent with those of Xie et al. (2016) who had observed that short-term GA treatment in *Populus tomentosa* induces an increase in photosynthesis activity, accompanied by 2- to 7.4-fold up-regulation of genes involved in the 'light reactions'. Furthermore, the free-GA content was significantly higher in rice accessions with BGlu-5 haplotype 1, as compared to accessions with BGlu-5 haplotype 2 and *bglu-5* KO transgenic lines (Fig. 6C), which is consistent with the hypothesis that the free-GA level might be related to the variation in F_v/F_m .

Does the observed natural variation of BGlu-5, and correspondingly that of F_v/F_m , affect plant performance? To answer this question, we studied the relationship between F_v/F_m and several agronomic traits, such as biomass, CO₂ assimilation and grain yield, using our rice mini-core collection (data not shown). Our results show that F_v/F_m was significantly negatively correlated with biomass (Table 2). In other words, the slight decrease in F_v/F_m , shown in BGlu-5 haplotype 2, was significantly associated with an increase in biomass. It is worth mentioning here that during the green revolution, the mutated SD1 gene, which results in decreased GA level and decreased F_v/F_m , was artificially selected in rice and barley (Sasaki et al. 2002, Spielmeier et al. 2002, Jia et al. 2009). Detailed study is needed in the future to elucidate the mechanistic linkage between the decrease in F_v/F_m and the increase in biomass production. It is worth mentioning that in the rice accessions used in this study, both in the 199 mini-core accessions and also the 3000

accessions, the BGlu-5 haplotype 1 is the majority of the haplotype (Tables S4 and File S5).

Conclusions

In the present study, we have applied GWAS as well as a transgenic approach to investigate potential genetic mechanisms underlying natural variation in F_v/F_m in a rice mini-core diversity panel. Our data suggest that *cis*-element polymorphism affecting the *BGlu-5* transcript level might have contributed to variation in F_v/F_m through a GA signaling pathway. Although we have focused on SNP1 in this study, the influence of other SNPs and genes on natural variation of F_v/F_m cannot be eliminated and will be examined in future studies. Here we emphasize that the GWAS technique can be used as a tool to mine genetic mechanisms controlling extremely conserved physiological parameters, as demonstrated here by the ability of this approach in mining genes controlling F_v/F_m , which is usually considered to be invariable across higher plants. Therefore, this study provides new support for using GWAS to study large arrays of physiological parameters and processes in plant biology, not only those with large genetic variation, but also those with high level of conservation between plants.

Author contributions

S.H. and X.-G.Z. conceived and conducted the experiments; S.H. performed most of the experiments; S.P., M.Q., N.K., J.J., M.L., X.L. and X.Z. provided technical assistance to S.H.; S.H., H.W. and G.Z. analyzed the data; G., C.C. and X.-G.Z. supervised the experiments; S.H. wrote most of the article; G., C.C. and X.-G.Z. supervised and complemented the writing.

Acknowledgement—The authors would like to thank the Chinese Academy of Sciences Strategic Research Project for financial support. Govindjee would like to thank the Department of Plant Biology, of the University of Illinois at Urbana-Champaign (UIUC) for providing office and Lab space. He gives special thanks to all the members of the staff of Information Technology, School of Integrative Biology and Molecular & Cell Biology, UIUC, for their help with the use of computers.

References

- Agrama HA, Yan WG, Lee F, Fjellstrom R, Chen MH, Jia M, McClung A (2009) Genetic assessment of a mini-core subset developed from the USDA Rice Genebank. *Crop Sci* 49: 1336–1346
- Araus JL, Amaro T, Voltas J, Nakkoul H, Nachit MM (1998) Chlorophyll fluorescence as a selection criterion for grain yield in durum wheat under Mediterranean conditions. *Field Crop Res* 55: 209–223
- Björkman O, Demmig B (1987) Photon yield of O₂ evolution and chlorophyll fluorescence characteristics at 77 K among vascular plants of diverse origins. *Planta* 170: 489–504
- Brzobohaty B, Moore I, Kristoffersen P, Bako L, Campos N, Schell J, Palme K (1993) Release of active cytokinin by a beta-glucosidase localized to the maize root meristem. *Science* 262: 1051–1054
- Butler WL (1978) Energy distribution in the photochemical apparatus of photosynthesis. *Annu Rev Plant Physiol* 29: 345–378
- Chapman EJ, Estelle M (2009) Mechanism of auxin-regulated gene expression in plants. *Annu Rev Genet* 43: 265–285
- Chen ML, Fu XM, Liu JQ, Ye TT, Hou SY, Huang YQ, Yuan BF, Wu Y, Feng YQ (2012) Highly sensitive and quantitative profiling of acidic phytohormones using derivatization approach coupled with nano-LC–ESI-Q-TOF-MS analysis. *J Chromatogr B* 905: 67–74
- Cong L, Ran FA, Cox D, Lin S, Barretto R, Habib N, Hsu PD, Wu X, Jiang W, Marraffini LA, Zhang F (2013) Multiplex genome engineering using CRISPR/Cas systems. *Science* 339: 819–823
- Cramer WA, Kallas T (eds)(2016) Cytochrome complexes: evolution, structures, energy transduction and signalling. In: *Advances in Photosynthesis and Respiration*. Springer, Dordrecht, pp 754
- Demmig-Adams B, Garab G, Adams WW, Govindjee (Eds)(2014) *Non-Photochemical Quenching of Chlorophyll a Fluorescence in Plants, Algae and Cyanobacteria*. Springer, Netherlands
- El-Lithy ME, Rodrigues GC, van Rensen JJ, Snel JF, Dassen HJ, Koornneef M, Jansen MA, Aarts MG, Vreugdenhil D (2005) Altered photosynthetic performance of a natural *Arabidopsis* accession is associated with atrazine resistance. *J Exp Bot* 56: 1625–1634
- Faraloni C, Cutino I, Petruccioli R, Leva AR, Lazzeri S, Torzillo G (2011) Chlorophyll fluorescence technique as a rapid tool for in vitro screening of olive cultivars (*Olea europaea* L.) tolerant to drought stress. *Environ Exp Bot* 73: 49–56
- Feng Z, Zhang B, Ding W, Liu X, Yang DL, Wei P, Cao F, Zhu S, Zhang F, Mao Y, Zhu JK (2013) Efficient genome editing in plants using a CRISPR/Cas system. *Cell Res* 23: 1229–1232
- Flood PJ, Harbinson J, Aarts MGM (2011) Natural genetic variation in plant photosynthesis. *Trends Plant Sci* 16: 327–335
- Flood PJ, Kruijer W, Schnabel SK, Schoor RVD, Jalink H, Snel JFH, Harbinson J, Aarts MGM (2016) Phenomics for photosynthesis, growth and reflectance in *Arabidopsis thaliana* reveals circadian and long-term fluctuations in heritability. *Plant Methods* 12: 1–14
- Gabriel SB, Schaffner SF, Nguyen H, Moore JM, Roy J, Blumenstiel B, Higgins J, DeFelice M, Lochner A, Faggart M, Liu-Cordero SN, Rotimi C, Adeyemo A, Cooper R, Ward R, Lander ES, Daly MJ, Altshuler D (2002) The structure of haplotype blocks in the human genome. *Science* 296: 2225–2229
- Garg AK, Kim JK, Owens TG, Ranwala AP, Choi YD, Kochian LV, Ray J, Wu RJ (2002) Trehalose accumulation in rice plants confers high tolerance levels to different abiotic stresses. *Proc Natl Acad Sci U S A* 99: 15898–15903
- Genty B, Briantais JM, Baker N (1989) The relationship between the quantum yield of photosynthetic electron transport and quenching of chlorophyll a fluorescence. *Biochim Biophys Acta* 990: 87–92
- Golbeck JH (ed) (2006) (Ed)Photosystem I: The Light-Induced Plastocyanin-Ferredoxin Oxido-Reductase. *Advances in Photosynthesis and Respiration*. Springer, Dordrecht
- Govindjee (1995) Sixty-three years since Kautsky: chlorophyll a fluorescence. *Aust J Plant Physiol* 22: 131–160
- Govindjee (2004) Chlorophyll a fluorescence: a bit of basics and history. In: Papageorgiou GC, Govindjee (eds) *Chlorophyll Fluorescence: A Signature of Photosynthesis*. Kluwer Academic, Dordrecht, pp 2–42
- Govindjee, Shevela D, Björn LO (2017) Evolution of the Z-scheme of photosynthesis. *Photosynth Res* 133: 5–15
- Hamdani S, Qu M, Xin C-P, Li M, Chu C, Govindjee, Zhu X-G (2015) Variations between the photosynthetic properties of elite and landrace Chinese rice cultivars revealed by simultaneous measurements of 820 nm transmission signal and chlorophyll a fluorescence induction. *J Plant Physiol* 177: 128–138
- Hedden P, Sponsel V (2015) A century of gibberellin research. *J Plant Growth Regul* 34: 740–760
- Huang X, Wei X, Sang T, Zhao Q, Feng Q, Zhao Y, Li C, Zhu C, Lu T, Zhang Z, Li M, Fan D, Guo Y, Wang A, Wang L, Deng L, Li W, Lu Y, Weng Q, Liu K, Huang T, Zhou T, Jing Y, Li W, Lin Z, Buckler ES, Qian Q, Zhang QF, Li J, Han B (2010) Genome-wide association studies of 14 agronomic traits in rice landraces. *Nat Genet* 42: 961–967
- Huang X, Zhao Y, Wei X, Li C, Wang A, Zhao Q, Li W, Guo Y, Deng L, Zhu C, Fan D, Lu Y, Weng Q, Liu K, Zhou T, Jing Y, Si L, Dong G, Huang T, Lu T, Feng Q, Qian Q, Li J, Han B (2012) Genome-wide association

- study of flowering time and grain yield traits in a world-wide collection of rice germplasm. *Nat Genet* 44: 32–39
- Jia Q, Zhang J, Westcott S, Zhang XQ, Bellgard M, Lance R, Li C (2009) GA-20 oxidase as a candidate for the semidwarf gene *sdw1/denso* in barley. *Funct Integr Genomics* 9: 255–262
- Kasajima I, Ebana K, Yamamoto T, Takahara K, Yano M, Kawai-Yamada M, Uchimiya H (2011) Molecular distinction in genetic regulation of nonphotochemical quenching in rice. *PNAS* 108: 13835–13840
- Kleczkowski K, Schell J (1995) Phytohormone conjugates: nature and function. *Crit Rev Plant Sci* 14: 283–298
- Klughammer C, Schreiber U (2008) Complementary PSII quantum yields calculated from simple fluorescence parameters measured by PAM fluorometry and the saturation pulse method. *PAM Appl Notes* 1: 27–35
- Kramer DM, Johnson G, Kiirats O, Edwards GE (2004) New flux parameters for the determination of QA redox state and excitation fluxes. *Photosynth Res* 79: 209–218
- Krause GH, Weis E (1984) Chlorophyll fluorescence as a tool in plant physiology. II. Interpretation of fluorescence signals. *Photosynth Res* 5: 139–157
- Kump KL, Bradbury PJ, Wisser RJ, Buckler ES, Belcher AR, Oropeza-Rosas MA, Zwonitzer JC, Kresovich S, McMullen MD, Ware D, Balint-Kurti PJ, Holland JB (2011) Genome-wide association study of quantitative resistance to southern leaf blight in the maize nested association mapping population. *Nat Genet* 43: 163–168
- Lawson T, David M, Kramer DM, Raines CA (2012) Improving yield by exploiting mechanisms underlying natural variation of photosynthesis. *Curr Opin Biotechnol* 23: 215–220
- Leister D (2012) How can the light reactions of photosynthesis be improved in plants? *Front Plant Sci* 3: 199. <https://doi.org/10.3389/fpls.2012.00199>
- Li RH, Guo PP, Baumz M, Grand S, Ceccarelli S (2006) Evaluation of chlorophyll content and fluorescence parameters as indicators of drought tolerance in barley. *Agric Sci China* 5: 751–757
- Liu H, Yang Y, Li H, Liu Q, Zhang J, Yin J, Chu S, Zhang X, Yu K, Lv L, Xi C, Zhang D (2018) Genome-wide association studies of photosynthetic traits related to phosphorus efficiency in soybean. *Front Plant Sci* 9: 1226–1235. <https://doi.org/10.3389/fpls.2018.01226>
- Livak K, Schmittgen TD (2001) Analysis of relative gene expression data using real-time quantitative PCR and the 2- $\Delta\Delta$ CT method. *Methods* 25: 402–408
- Luo A, Qian Q, Yin H, Liu X, Yin C, Lan Y, Tang J, Tang Z, Cao S, Wang X, Xia K, Fu X, Luo D, Chu C (2006) EU11, encoding a putative cytochrome P450 monooxygenase, regulates internode elongation by modulating gibberellin responses in rice. *Plant Cell Physiol* 47: 91
- Ma X, Chen L, Zhu Q, Chen Y, Liu YG (2015) Rapid decoding of sequence-specific nuclease-induced heterozygous and biallelic mutations by direct sequencing of PCR products. *Mol Plant* 8: 1285–1287
- Mamedov M, Govindjee, Nadochenko V, Semenov A (2015) Primary electron transfer processes in photosynthetic reaction centers from oxygenic organisms. *Photosynth Res* 125: 51–63
- Mirkovic T, Ostrumov EE, Anna JM, van Grondelle R, Govindjee, Scholes GD (2017) Light absorption and energy transfer in the antenna complexes of photosynthetic organisms. *Chem Rev* 117: 249–293
- Nelson N, Yocum CF (2006) Structure and function of photosystems I and II. *Annu Rev Plant Biol* 57: 521–565
- Nishimura A, Aichi I, Matsuoka M (2006) A protocol for agrobacterium-mediated transformation in rice. *Nat Protoc* 1: 2796–2802
- Ortiz D, Hu J, Fernandez MGS (2017) Genetic architecture of photosynthesis in *Sorghum bicolor* under non-stress and cold stress conditions. *J Exp Bot* 68: 4545–4557
- Papageorgiou GC, Govindjee (Eds)(2004) Chlorophyll a Fluorescence: A Signature of Photosynthesis. Springer, Netherlands
- Qu M, Zheng G, Hamdani S, Essmine J, Song Q, Wang H, Chu C, Sirault X, Zhu XG (2017) Leaf photosynthetic parameters related to biomass accumulation in a 2 global rice diversity survey. *Plant Physiol* 175: 248–258. <https://doi.org/10.1104/pp.17.00332>
- Sasaki A, Ashikari M, Ueguchi-Tanaka M, Itoh H, Nishimura A, Swapan D, Ishiyama K, Saito T, Kobayashi M, Khush GS, Kitano H, Matsuoka M (2002) Green revolution: a mutant gibberellin-synthesis gene in rice. *Nature* 416: 701–702
- Spielmeier W, Ellis MH, Chandler PM (2002) Semidwarf (*sd-1*), “green revolution” rice, contains a defective gibberellin 20-oxidase gene. *Proc Natl Acad Sci U S A* 99: 9043–9048
- Srivastava A, Guisse B, Greppin H, Strasser RJ (1997) Regulation of antenna structure and electron transport in photosystem II of *Pisum sativum* under elevated temperature probed by the fast polyphasic chlorophyll a fluorescence transient: OKJIP. *Biochim Biophys Acta* 1320: 95–106
- Stirbet A, Govindjee (2011) On the relation between the Kautsky effect (chlorophyll a fluorescence induction) and photosystem II: basics and applications of the OJIP fluorescence transient. *J Photochem Photobiol B* 104: 236–257
- Tian F, Bradbury PJ, Brown PJ, Hung H, Sun Q, Flint-Garcia S, Rocheford TR, McMullen MD, Holland JB, Buckler ES (2011) Genome-wide association study of leaf architecture in the maize nested association mapping population. *Nat Genet* 43: 159–162
- Tong H, Xiao Y, Liu D, Gao S, Liu L, Yin Y, Jin Y, Qian Q, Chu C (2014) Brassinosteroid regulates cell elongation by modulating gibberellin metabolism in rice. *Plant Cell* 26: 4376–4393

- Wang D, Sun Y, Stang P, Berlin JA, Wilcox MA, Li Q (2009) Comparison of methods for correcting population stratification in a genome-wide association study of rheumatoid arthritis: principal-component analysis versus multidimensional scaling. *BMC Proc* 3: S109. <https://doi.org/10.1186/1753-6561-3-S7-S109>
- Wang H, Xu X, Vieira FG, Xiao Y, Li Z, Wang J, Nielsen R, Chu C (2016) The power of inbreeding: NGS-based GWAS of rice reveals convergent evolution during rice domestication. *Mol Plant* 9: 975–985
- Wiese G, Grambow HJ (1986) Indole-3-methanol-b-D-glucoside and indole-3-carboxylic acid-b-glucoside are products of indole-3-acetic acid degradation in wheat leaf segments. *Phytochemistry* 25: 2451–2455
- Wydrzynski T, Satoh K (eds) (2005) (Eds) Photosystem II: The Light-Induced Water-Plastoquinone Oxido-Reductase. *Advances in Photosynthesis and Respiration*. Springer, Dordrecht
- Xie J, Tian J, Du Q, Chen J, Li Y, Yang X, Li B, Zhang D (2016) Association genetics and transcriptome analysis reveal a gibberellin-responsive pathway involved in regulating photosynthesis. *J Exp Bot* 67: 3325–3338. <https://doi.org/10.1093/jxb/erw151>
- Xin CP, Yang J, Zhu XG (2013) A model of chlorophyll a fluorescence induction kinetics with explicit description of structural constraints of individual photosystem II units. *Photosynth Res* 117: 339–354
- Yamane Y, Kashino Y, Koike H, Satoh K (1998) Effects of high temperatures on the photosynthetic systems in spinach: oxygen-evolving activities, fluorescence characteristics and the denaturation process. *Photosynth Res* 57: 51–59
- Yin Z, Meng F, Song H, He X, Xu X, Yu D (2010) Mapping quantitative trait loci associated with chlorophyll a fluorescence parameters in soybean (*Glycine max* (L.) Merr.). *Planta* 231: 875–885
- Zhao K, Tung CW, Eizenga GC, Wright MH, M Ali ML, Price AH, Norton GJ, Islam MR, Reynolds A, Mezey J, McClung AM, Bustamante CD, Susan R, SR MC (2011) Genome wide association mapping reveals a rich genetic architecture of complex traits in *Oryza sativa*. *Nat Commun* 2: 467
- Zubo YO, Yamburenko MV, Selivankina SY, Shakirova FM, Avalbaev AM, Kudryakova NV, Zubkova NK, Liere K, Kulaeva ON, Kusnetsov VV, Börner T (2008) Cytokinin stimulates chloroplast transcription in detached barley leaves. *Plant Physiol* 148: 1082–1093

Supporting Information

Additional supporting information may be found online in the Supporting Information section at the end of the article.

Fig. S1. Effect of far-red pre-illumination in F_0 and F_v/F_m values.

Fig. S2. Structure of the CRISPR/Cas9 binary vector pBKG032.

Fig. S3. Map showing geographical distribution for our rice mini-core collection (199 accessions).

Fig. S4. Sequence alignment of target gene between homozygous mutants (obtained using CRISPR/Cas 9 method) and wild type.

Table S1. Primers used for gene amplification and qRT-PCR analysis.

Table S2. List of significant SNPs and the surrounding genes.

Table S3. Allelic diversities of SNPs and the corresponding F_v/F_m

Table S4. The allelic variations of SNP in 3000 rice accessions.

Table S5. The number of accessions in different haplotypes in the 3000 rice accessions.